X-RAY SPECTROMETRY, VOL. 16, 181-185 (1987)

Description of Low-Energy Peak Distortion Observed in X-Ray Spectrometry with Si(Li) Detectors

J. Heckel
Technische Universität Dresden, Sektion Physik, Bereich AKP, Mommsenstr. 13, Dresden 8027, GDR

W. Scholz
Zentrum für wissenschaftlichen Gerätebau der AdW der DDR, Schnellerstr. 138, Berlin 1190, GDR

A simple model is developed to describe the shape and intensity of the low-energy peak distortion measured with Si(Li) detectors in x-ray spectrometry. Based on this model, a method is outlined for correcting the distortion channel by channel, which drastically reduces the expense of the deconvolution of the pulse-height spectra measured in energy-dispersive x-ray emission analysis with Si(Li) detectors.

INTRODUCTION

Quantitative elemental analysis performed with energy-dispersive x-ray spectrometers with Si(Li) detectors requires the accurate estimation of the sample composition from the extraction of net intensities in the measured pulse-height spectrum. For systems in which the electronics are highly stable one can successfully apply the method of approximation of standard spectra.[1,2] However, Russ[2] pointed out that an analytical procedure can only achieve high flexibility and universality if it includes the generation and approximation of analytical peak models for estimating the desired net intensities. The peak shape is considered to be a Lorentzian distribution folded with a Gaussian.[3] Deviations from this ideal shape due to additional detector effects are further referred to as peak distortions.

In recent years, a number of analytical models have been discussed, especially with regard to the peak distortions due to incomplete charge collection (e.g. Refs 4-6). The basic model of the response function is a Gaussian distribution with additional parametric functions to describe the incomplete charge collection effects. Together with the basic parameters, the parameters of the distortion function are iteratively optimized to fulfil the least-squares demands.[6]

A recurrence relationship was used by Arthur *et al.*[7] to subtract the distortion parts from the spectrum channel by channel. The parameters included in this model are predicted by some preliminary experiments. The advantage of this method is a drastic reduction in computation time and a simplification of the peak model, because simple Gaussian distributions can be used to describe the peaks after removal of distortions. Joy[8] used a physical model which includes detector parameters such as recombination velocity and diffusion length of charge carriers to compute low-energy peak shapes. The results were applied to the microanalysis of light elements.

In this work, a similar method was used to consider the effects of incomplete charge collection. Based on simple physical models, a response function is developed to describe the behaviour of Si(Li) detectors with Schottky surface barriers used in energy-dispersive x-ray spectrometry. The response function was applied to the channel by channel correction of peak distortions.

EXPERIMENTAL

The spectra were obtained with a Kevex 7000 Si(Li) detector attached to an ARL microprobe. The integral count rates were below 2000 counts s^{-1} and counting times of 200-1000 s were used. The spectra were processed with a minicomputer using the special software package UNI-ZAF developed by the authors.

Observations

Figure 1 shows a spectrum of an iron-55 nuclide source. The visible distortion of the characteristic lines of Mn can be subdivided into three parts: the escape lines, a nearly constant background extending from zero up to the line energy and a distortion of the low-energy shoulder of the peaks. The first two parts of the distortion can be corrected in a straightforward manner.[9,10] In the following we only consider the third part of the distortion.

The effect of incomplete charge collection also results in a distortion of the bremsstrahlung spectrum in x-ray microanalysis at the energy of Si K-absorption edge as shown by Fiori *et al.*[11]

THEORY

Mathematical description of the measurement

In energy-dispersive x-ray spectrometry the measurement can be described by the following convolution

0049-8246/87/040181-05$05.00
© 1987 by John Wiley & Sons, Ltd.
Received 5 September 1986
Revised 10 March 1987

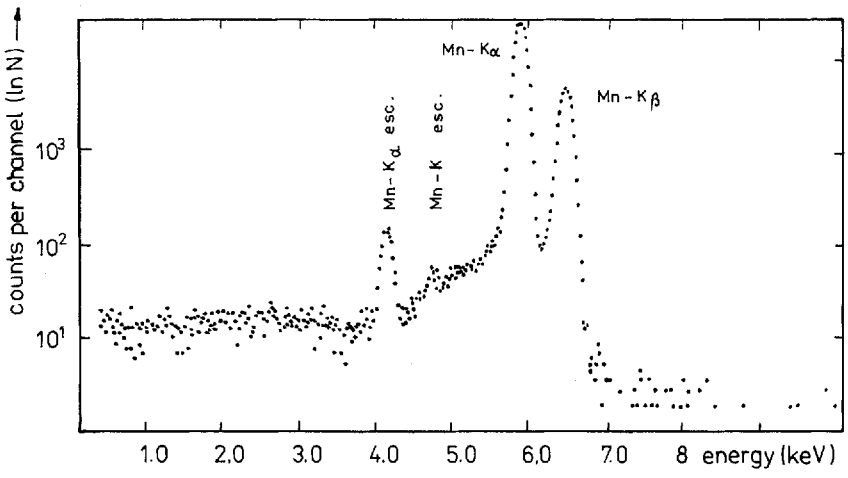

Figure 1. Pulse-height spectrum of an iron-55 source.

integral:

$$M(E') = \int T(E)R(E, E')\mathrm{d}E + N(E) \qquad (1)$$

where $M(E')$ = measured pulse-height spectrum; $T(E)$ = line spectrum emitted by the sample; $R(E, E')$ = response function of the spectrometer; $N(E')$ = statistical noise component; E = energy of photons.

The response function takes into account the absorption and transmission properties of the spectrometer and thus predicts the peak shape in the pulse-height spectrum. By neglecting the natural line widths, the emission spectrum can be represented by a sum of Dirac δ-functions and so the response function also contains properties of the detector which lead to distortion distributions on the low-energy side of a peak, further referred to as peak distortions.

To simplify matters we separate the response function into a Gaussian and a distortion function:

$$R(E, E') = G(E, E') * D(E, E') \qquad (2)$$

(the asterisk represents the mathematical convolution). The statistics of charge creation in the detector and the noise of the electronics are described by the Gaussian part. The distortion function $D(E, E')$ characterizes the effects of incomplete charge collection.

Model of the distortion function $D(E, E')$

In recent years, a number of models have been presented to explain the peak distortions (e.g. Refs 12-15). The basic properties of semiconductor detectors were discussed in terms of sources of distortion such as the diffusion of charge carriers and the structure of the detector. However, Nagai *et al.*[14] showed that the proposed models are not sufficient for a complete and consistent explanation of the distortions.

Figure 2 shows the principle of an Si(Li) detector. A photon absorbed in the detector creates n_G electron-hole pairs on average:

$$n_G = \frac{h\nu}{\varepsilon} \qquad (3)$$

where ε is the average energy to create one pair and its value is 3.92 eV for silicon at 77 K.[16] The electron-hole

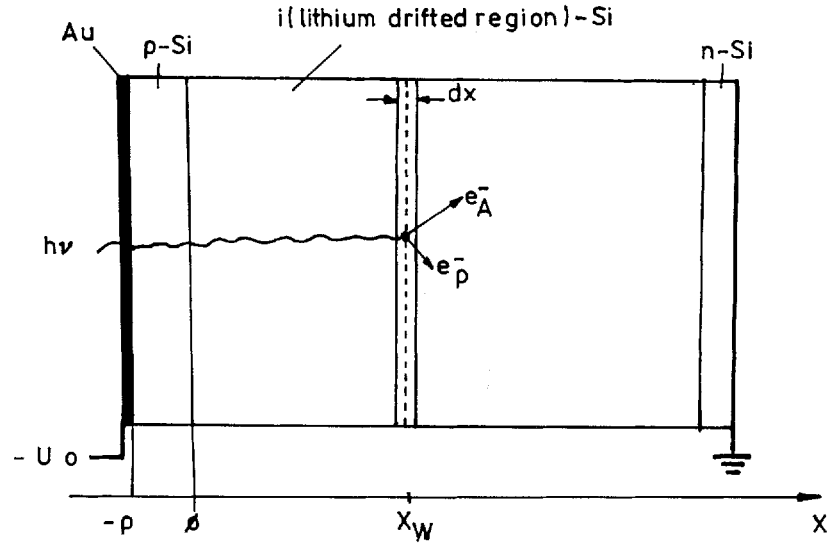

Figure 2. Principle of an Si(Li) detector, including schematic representation of a photoionization at position x_W within a layer of thickness dx.

pairs are collected by an electrical field (voltage 500–2000 V), only those in the intrinsic region being collected. Incomplete charge collection occurs when charge carriers recombine in the field-free p-layer.

The problem is to predict the number, n_V, of charge carrier pairs situated in the p-layer when collection takes place depending on the position of the primary interaction of the incident photon with the detector material. The remainder of these pairs, $n_S = n_G - n_V$, leads to a pulse in the peak distortion.

The description of the interactions in the detector is divided into three subprocesses. We consider only the collection of electrons.

Creation of primary electrons. A photoelectron is created by the photoabsorption of a photon in the detector at position x_W in a layer of thickness dx (in the following we consider only K and L photoelectrons). After de-excitation, e.g. of a K vacancy, an Auger electron occurs with a probability of 95%. Scattering of photons is neglected because the photoabsorption coefficient of Si and the mass attenuation coefficient of Si are nearly identical for the considered energy region of 1–10 keV.

The escape of the Si K-photon is well described by the known escape effect,[10] so we can further consider only photo- and Auger electrons.

The energy E_{PK} of a K-photoelectron is

$$E_{PK}\,(\text{keV}) = h\nu - 1.84 \tag{4}$$

and the energy E_{PL} of an L-photoelectron is on average

$$E_{PL}\,(\text{keV}) = h\nu - 0.1 \tag{5}$$

For the energy of the KLL Auger electrons we assume a mean value of $E_A = 1.66$ keV. If the anisotropy of the emission direction of the electrons is neglected, then the range factor describes a spherical surface. The range can be estimated according to Fitting[17] by

$$R\,(\text{nm}) = 90\rho^{-0.8}E^{1.3} \tag{6}$$

where ρ g cm^{-1} is the density of the material (here Si) and E keV is the primary energy of the electrons.

Production of hot charge carriers. The second subprocess contains all interactions caused by the primary electrons along their stopping path. These interactions produce a number of electron–hole pairs proportional to the primary photon energy according to Eqn (3).

To consider the effects of electron backscattering, a Gaussian distribution is assumed to describe the radial density of the hot electron distribution. It can be clearly seen in Fig. 2 that the position of the centre along the abscissa is decisive for collection loss in the p-layer. Therefore, we consider two cases: (a) the maximum collection loss is to be expected if the primary electron is emitted in a direction towards the p-layer parallel to the abscissa; and (b) the minimum collection loss will occur if the direction is the opposite to that in (a). All other directions of emission between these two cases are considered as to be equally distributed.

Thermalizing of hot electrons. As shown by Llacer *et al.*,[15] with Ge detectors the average free path length of electrons will increase with decreasing electron energy independently of the applied voltage of the detector. This increase is the reason for the extension of a region in the detector in which incomplete charge collection can occur after a primary ionization. This region is generally designated as the 'dead layer' of the detector.

For a simplified description of thermalization the diffusion model is used. With the help of this model, Goulding[12] obtained results similar to those of Llacer *et al.*[15] for the estimated dead layers.

If the diffusing electron distribution reaches the Schottky surface barrier at $x = -p$, we assume that the reflection probability is 100%. After a relaxation time τ, the electric field begins to effect and collects all charge carriers located in the i-region of the detector. The electron loss and hence the energy loss of the primary electrons, subdivided into cases (a) and (b) above, can be estimated by integration of the density distribution within the p-Si layer.

RESULTS

In a computer experiment, all subprocesses explained above are computed in detector layers dx, at interaction points $-p < x_W < x_{max}$, whereby at x_{max} no losses can occur.

In Fig. 3 some computed functions $N(E_{h\nu}, E')$ are shown for element-specific photon energies. With the help of measured spectra, the value $D\tau$ (D = diffusion constant) was optimized. The only free parameter is then the thickness of the p-Si layer, which directly defines the low energy limit of the distortion distribution. A functional dependence is shown in Fig. 4. For the detector used for the measurements, the following values were found: thickness of p-Si layer = 0.014 μm and thickness of dead layer = 0.24 μm.

APPLICATION

With the help of the optimized functions $N(E_{h\nu}, E')$ we can correct the measured spectra. An example is shown in Fig. 5.

Beginning at the high-energy end of the pulse-height spectrum, the function $N(E_{h\nu}, E')$ is normalized to the actual channel and is subtracted from the measured spectrum. The sum of all pulses subtracted is added to the normalization channel. This is repeated up to the low-energy end of the spectrum.

An approximation of two Gaussians to the Cl $K\alpha_{1,2}$ line and to the Cl K_β line gives a value for the figure of merit $\chi^2_R = 2.3$ within the peak region. Without any distortion correction, a value of $\chi^2_R = 8.9$ was obtained.

With the suggested method the accuracy of deconvolution can be improved. Normally, the optimized function $N(E_{h\nu}, E')$ should be included in the peak model to perform a more accurate deconvolution. However, in most cases in x-ray microanalysis there are no further improvements in comparison with the previous method.

For investigation of the fine structure of peak shapes, the channel by channel correction method is not usable. For practical application of the function $N(E_{h\nu}, E')$ the

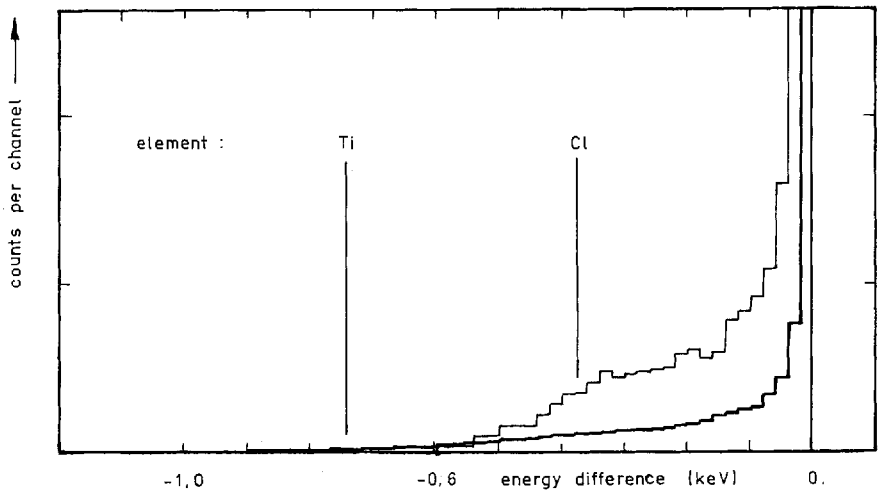

Figure 3. Computed distortion distributions for different primary photon energies.

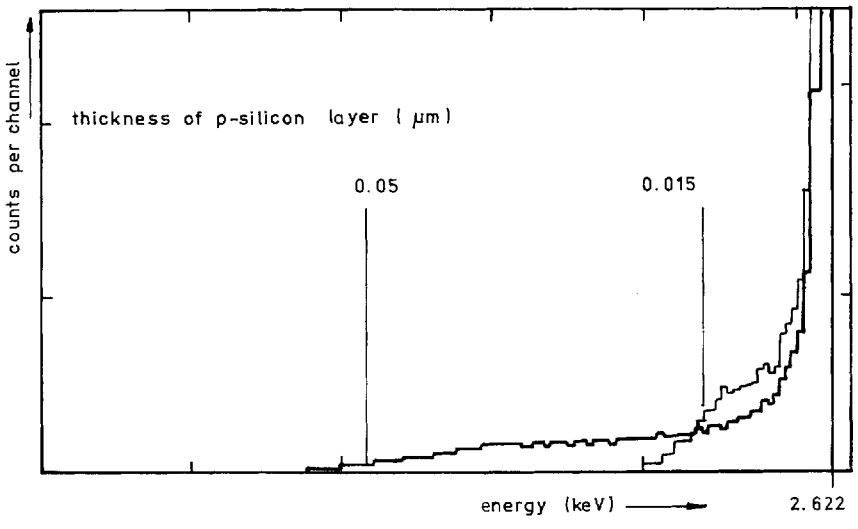

Figure 4. Computed distortion distributions for different thicknesses of p-Si layers.

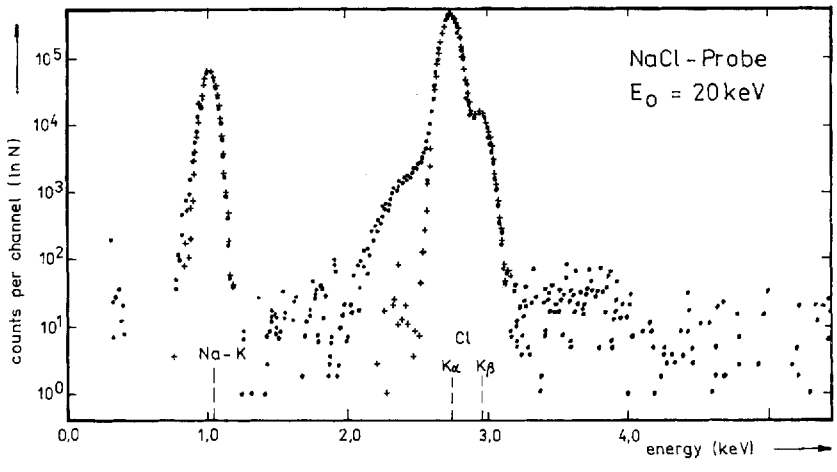

Figure 5. Background-corrected NaCl pulse-height spectrum before (•) and after (+) distortion correction.

structure of this function was normalized in a suitable manner and was stored in a table in order to avoid the repeated computation of the function.

The CPU times necessary for correcting the K series of Cl and to approximate two Gaussians to estimate the net intensity of the Cl $K\alpha_{1,2}$ line are nearly two orders of magnitude smaller than a complete χ^2 parameter optimization of $G(E_{h\nu}, E')$ and $D(E_{h\nu}, E')$ in Eqn (2).

Acknowledgements

We thank Prof. G. Musiol and Prof. N. Langhoff for promoting the paper and Dr H. Baum for supporting the experimental work.

REFERENCES

1. J. J. McCarthy and F. H. Schamber, in *Proceedings of the Workshop on Energy Dispersive X-ray Spectrometry, Gaithersburg, April 1979*, edited by K. F. J. Heinrich *et al.*, NBS SP 604. National Bureau of Standards, Washington, DC (1981).
2. J. C. Russ in *Proceedings of the Workshop on Energy Dispersive X-ray Spectrometry, Gaithersburg, April 1979*, edited by K. F. J. Heinrich *et al.*, NBS SP 604. National Bureau of Standards, Washington, DC (1981).
3. C. W. Schulte, H. H. Jorch and J. L. Campbell, *Nucl. Instrum. Methods* **174**, 549 (1980).
4. H. H. Jorch and J. L. Campbell, *Nucl. Instrum. Methods* **143**, 551 (1977).
5. J. L. Campbell, B. M. Hillman, J. A. Maxwell, A. Perujo and W. J. Teesdale, *Nucl. Instrum. Methods* **B9**, 71 (1985).
6. E. Marageter, W. Wegscheider and K. Mueller, *Nucl. Instrum. Methods* **B1** 137 (1984).
7. R. J. Arthur, M. W. Hill and N. F. Mangelson, *Nucl. Instrum. Methods* **B3** 305 (1984).
8. D. C. Joy, *Rev. Scient. Instrum.* **56**, 1772 (1985).
9. H. D. Keith and T. C. Loomis, *X-Ray Spectrom.* **5**, 93 (1975).
10. S. J. B. Reed and N. G. Ware, *X-Ray Spectrom.* **2**, 69 (1973).
11. C. E. Fiori, D. E. Newbury and R. L. Myklebust, in *Proceedings of the Workshop on Energy Dispersive X-ray Spectrometry, Gaithersburg, April 1979*, edited by K. F. J. Heinrich *et al.*, NBS SP 604. National Bureau of Standards, Washington, DC (1981).
12. F. S. Goulding, *Nucl. Instrum. Methods* **142**, 213 (1977).
13. K. Shima, S. Nagai and T. Mikumo, *Nucl. Instrum. Methods* **217**, 515 (1983).
14. S. Nagai, T. Ogami, M. Okibara, M. Oka, K. Shima and T. Mikumo, *Radioisotopes* **33**, 119 (1984).
15. J. Llacer, E. E. Haller and R. C. Cordi, *IEEE Trans. Nucl. Sci.* **NS-24**, 53 (1977).
16. D. W. Aitken, *IEEE Trans. Nucl. Sci.* **NS-15**, 10 (1968).
17. H.-J. Fitting, *Phys. Status Solidi A* **26**, 525 (1974).